JOURNAL OF COMPUTATIONAL PHYSICS 76, 176–191 (1988)

Computer Simulation Results for the Two-Point Probability Function of Composite Media

P. SMITH

Department of Mechanical and Aerospace Engineering, North Carolina State University, Raleigh, North Carolina 27695-7910

AND

S. TORQUATO*

Departments of Mechanical and Aerospace Engineering and of Chemical Engineering, North Carolina State University, Raleigh, North Carolina 27695-7910

Received April 30, 1987, revised July 9, 1987

Computer simulation results are reported for the two-point matrix probability function S_2 of two-phase random media composed of disks distributed with an arbitrary degree of impenetrability λ. The novel technique employed to sample $S_2(r)$ (which gives the probability of finding the endpoints of a line segment of length r in the matrix) is very accurate and has a fast execution time. Results for the limiting cases $\lambda = 0$ (fully penetrable disks) and $\lambda = 1$ (hard disks), respectively, compare very favorably with theoretical predictions made by Torquato and Beasley and by Torquato and Lado. Results are also reported for several values of λ that lie between these two extremes, cases which heretofore have not been examined. © 1988 Academic Press, Inc

I. INTRODUCTION

A wide class of two-phase random media, such as suspensions, porous media, and composite materials, are composed of discrete particles which are randomly distributed throughout another phase, generically referred to as the matrix phase (fluid, solid, or void). A fundamental understanding of the bulk properties (conductivity, elastic moduli, fluid permeability, etc.) of such materials rests upon knowledge of distribution functions that statistically characterize the microstructure [1]. In particular, such media can be characterized by the set of n-point matrix probability functions S_n, which give the probability of finding n points all in the matrix phase. The lower order functions S_1, S_2, and S_3 arise in rigorous bounds on the conductivity [2, 3] and elastic moduli [4, 5] of composite media, rate constant

* To whom all correspondence should be addressed

0021-9991/88 $3.00

of diffusion-controlled reactions in porous media [6], and the fluid permeability of porous media [6–8].

In a series of recent papers [9–13], Torquato and Stell developed a theoretical formalism which enables one to compute the S_n for media composed of particles such that the location of each inclusion is fully specified by a center-of-mass coordinate (e.g., spheres, disks, and oriented cubes, squares and ellipsoids). It is only very recently, however, that computer-simulation techniques have been employed to generate S_1, S_2, and S_3 [14–16] for models of random media.

This paper reports computer simulation results for S_2 of two-dimensional (2D) media composed of (possibly overlapping) disks of equal radius R in a matrix. Our interest in 2D materials is twofold. First, certain 2D media (such as distributions of impenetrable disks) are useful models of fiber-reinforced materials. Second, since the salient qualitative behavior of the function S_2 is not strongly affected by a change in the dimensionality of the system [17], simulation results obtained for 2D models (which are clearly less costly than 3D simulations) can be employed to infer the qualitative behavior of S_2 for analogous 3D models. The simulation method presented here, moreover, can easily be extended to 3D media.

In this study, we seek to investigate the effect of interparticle connectedness on S_2 for isotropic distributions of disks in the penetrable-concentric-shell (PCS) model introduced by Torquato [18]. (The degree of the connectivity of the constitutive phases may dramatically influence the transport and mechanical properties of two-phase media, particularly when the phase properties differ significantly [19].) Interparticle connectedness in the PCS model is related to the degree of penetrability $1-\lambda$ of the disks ($0 \leqslant \lambda \leqslant 1$); $\lambda = 0$ and $\lambda = 1$ corresponding to the limiting cases of "fully penetrable" and "totally impenetrable" disks, respectively. The novel technique presented here to sample for S_2 is not only accurate but has a fast execution time.

This article is organized as follows. In Section II, we define S_2 and describe our model system. In Section III, we present our method for calculating S_2 from computer simulations. In Section IV, we report results for S_2 in the PCS model for $\lambda = 0$, 0.5, 0.7, 0.9, and 1 at various particle-phase volume fractions. The results for $\lambda = 0$ and $\lambda = 1$ are compared to known theoretical results. Finally, in Section V, we make concluding remarks.

II Two-Point Function and Model System

A. *Two-Point Function* S_2

For any two-phase random medium, we define the following characteristic function for one of the phases, say phase 1,

$$I(\mathbf{r}) = \begin{cases} 1, & \text{if } \mathbf{r} \text{ is in phase 1,} \\ 0, & \text{if } \mathbf{r} \text{ is in phase 2,} \end{cases} \tag{1}$$

where $\mathbf{r}$ is a position vector within the macroscopic sample. The one- and two-point probability functions for phase 1 are then defined by [9]

$$S_1(\mathbf{r}_1) = \langle I(\mathbf{r}_1) \rangle, \tag{2}$$

$$S_2(\mathbf{r}_1, \mathbf{r}_2) = \langle I(\mathbf{r}_1)\, I(\mathbf{r}_2) \rangle, \tag{3}$$

where angular brackets denote an ensemble average. For statistically homogeneous media, S_1 is simply equal to the volume fraction ϕ_1 of phase 1 and $S_2(\mathbf{r})$ depends only on the relative position $\mathbf{r} = \mathbf{r}_2 - \mathbf{r}_1$. If, in addition, the medium is statistically isotropic, then $S_2(\mathbf{r})$ depends on the relative distance $r = |\mathbf{r}|$. In general, for statistically homogeneous media, S_2 has the asymptotic properties

$$S_2(0) = S_1 = \phi_1, \tag{4}$$

$$\lim_{r \to \infty} S_2(r) = \phi_1^2. \tag{5}$$

Equation (4) follows from definitions (2) and (3). Condition (5) assumes the system possesses no long-range order.

The specific surface s (interfacial surface area per unit volume) for isotropic 3D media has been related to the slope of $S_2(r)$ at $r = 0$ by Debye, Anderson, and Brumberger [20]. By generalizing their arguments to 2D media, we find for isotropic 2D two-phase systems that

$$s = -\pi \left. \frac{dS_2(r)}{dr} \right|_{r=0}. \tag{6}$$

A variety of transport properties depend upon s, including the rate constant associated with chemical reactions in porous media [7] and the fluid permeability of porous materials [7, 8, 21].

B. *Model System*

We consider computing $S_2(r)$ for isotropic distributions of equisized disks at a number density ρ in the PCS model [18]. Hence if phase 1 denotes the matrix phase, then ϕ_1 is the matrix volume fraction, ϕ_2 is the particle-phase (or simply disk) volume fraction, and $S_2(r)$ gives the probability of finding the endpoints of a line segment of length r in the matrix. In the PCS model (depicted in Fig. 1), disks (or parallel cylinders) of radius R are statistically distributed throughout a matrix subject only to the condition of a mutually impenetrable core of radius λR; λ being the impenetrability parameter, $0 \leqslant \lambda \leqslant 1$. Each disk of radius R, therefore, is composed of an impenetrable core of radius λR, encompassed by a perfectly penetrable concentric shell of thickness $(1 - \lambda)\, R$. It is clear that the limiting cases $\lambda = 0$ and $\lambda = 1$ correspond, respectively, to "fully penetrable" disks (in which disk centers are completely uncorrelated) and "totally impenetrable" disks. The PCS model for $\lambda \sim 1$, serves as a useful model of fiber-reinforced materials with oriented, con-

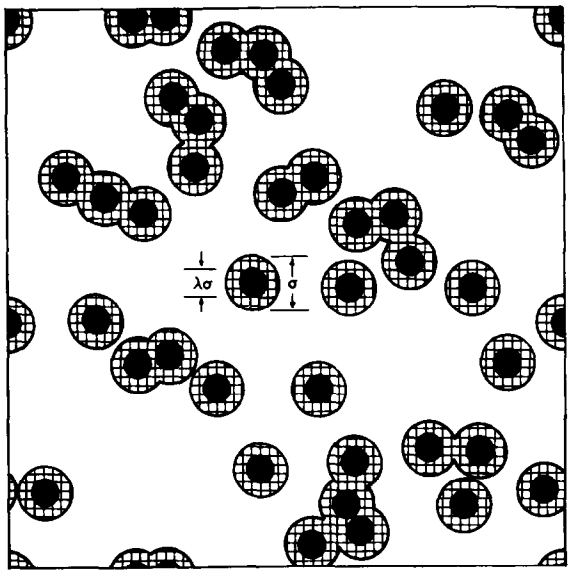

FIG 1 A computer-generated realization of a distribution of disks of radius $R = \sigma/2$ (shaded region) in a matrix (unshaded region) in the PCS model [18] The disks have an impenetrable core of diameter $\lambda\sigma$ indicated by the smaller, black circular regions Here $\lambda = 0\,5$ and the particle volume fraction $\phi_2 = 0\,3$

tinuous fibers and of thin films [22]. The 3D analog of the PCS model (involving spheres) for $\lambda < 1$ is a good model of consolidated media such as sandstones and sintered materials [19].

For $\lambda > 0$ (i.e., for finite-sized hard cores), the impenetrability condition alone does not uniquely determine the distribution. One may assume an equilibrium distribution [13, 17] or some nonequilibrium distribution, such as random sequential addition (RSA) [23]. The equilibrium and RSA distributions are known to be different at the same number density ρ [23]. Computer simulation results reported in Section IV are for RSA.

In RSA, configurations are generated by randomly and sequentially placing particles in a unit cell. As each particle is added, it is determined whether the hard cores (of radius λR) overlap with any other hard core already in the unit cell. If the hard cores overlap, then that particular particle is removed and added again until it finds a vacancy. Ultimately, so many particles are added that a next particle finds no accessible space. This is the jammed state. The jamming limit for RSA distributions of *totally impenetrable* disks ($\lambda = 1$) occurs at $\phi_2 \simeq 0.55$ [24, 25], which is well below the close-packing limit of $\phi_2 \simeq 0.82$ [26] for equilibrium distributions.

For the special case of fully penetrable disks ($\lambda = 0$), the distribution is uniquely determined by virtue of the total lack of spatial correlation between disk centers. In this limit, the n-point matrix probability functions have an especially simple analytical form. For example, for a distribution of fully penetrable disks at reduced

number density $\eta = \rho A_1$ (where $A_1 = \pi R^2$ is the area of one disk), the one- and two-point functions are given by [22]

$$S_1 = \phi_1 = \exp[-\eta], \tag{7}$$

$$S_2(r) = \exp[-\eta A_2(r)/A_1], \tag{8}$$

where

$$\frac{A_2(x)}{A_1} = 2 - \frac{2}{\pi}\left[\frac{\pi}{2} - \sin^{-1} x - x(1-x^2)^{1/2}\right] H(1-x) \tag{9}$$

is the union area of two disks of diameter $\sigma = 2R$ whose centers are separated by a distance r ($x = r/\sigma$). Here $H(x)$ is the Heaviside step function equal to unity for $x > 0$ and zero otherwise. Use of (8) and (9) gives the specific surface for $\lambda = 0$:

$$s = \frac{2}{R}\eta\phi_1. \tag{10}$$

Equations (8) and (10) will serve as useful checks on our simulation results.

Before closing this section, it is important to note that the disk volume fraction $\phi_2 = 1 - \phi_1$ is equal to the reduced density $\eta = \rho A_1$ only for the specific case of totally impenetrable disks ($\lambda = 1$). In general, at the same reduced density η, $\phi_2(\lambda) \leqslant \phi_2(\lambda = 1) = \eta$ and $s(\lambda) \leqslant s(\lambda = 1) = 2\eta/R$, for $0 \leqslant \lambda \leqslant 1$.

III. Simulation Procedure

A. *Preliminary Discussion*

Obtaining $S_2(r)$ from computer simulations is a two-step process. First of all, one must generate realizations of the random medium. Subsequently, one samples each realization for the two-point function and then averages over a sufficiently large number of realizations to obtain $S_2(r)$. We are specifically interested in computing $S_2(r)$ for RSA distributions of disks in the PCS model at specified disk volume fraction ϕ_2 and impenetrability index λ. In general, the methods available for storing images of configurations of particles are: (1) a bit-mapped (digitized) image, (2) an object-oriented approach (defined below), or (3) some hybrid of the preceeding two methods. In each case, in order to simulate an infinite system, one surrounds the image with replicas of itself, i.e., periodic boundary conditions (PBC) are employed.

When a bit-mapped approach is used, disks are "painted" onto a large square grid (pixel array) by setting all bits inside the disks (and hence in the particle phase) to 1. Initially, all bits are zeroed (100 % matrix phase) Note that only phase information is retained i.e., the disks lose any individual identity. The error introduced when representing objects in this manner diminishes as we increase the

number of pixels We shall refer to this approach as the GRID method. This is the method that we employ in this study

Berryman [14] used the GRID method (with a resolution of 512×512 pixels) to digitally process a single photograph of a synthetic composite material. He calculated lower-order spatial correlation functions using Fourier transform methods and array processing techniques; he then calculated effective property bounds. It is important to note that Berryman obtained correlation functions using only a single realization of each material. Recently, Berryman and Blair [21] employed this technique to ascertain S_2 for real porous-medium samples.

When an object-oriented approach is used, the coordinates of the centers of each disk (plus any periodic images within a specified cutoff distance) are stored. If the disks are of unequal size, then the radius of each disk must be stored as well. Note that the particles do not lose their individual identities. We shall refer to this approach as the "stored-configuration" (SC) method. Monte Carlo [27] and molecular dynamics [28] techniques used in the study of the liquid state are examples of the SC method.

Configuration generation with the GRID method is slower than with the SC method for circular disks. This is because many pixels must be manipulated with the GRID method. In our simulations, we use disks of radius $R = 0.03$. This means that there are (with 1024×1024 resolution) approximately 2965 bits within each disk and that each disk is circumscribed by a square of side of length 0.06 that contains approximately 3775 bits. Figure 2 shows totally impenetrable disks ($R = 0.03$) with the coarser 512×512 resolution (771 bits per disk), at a disk volume fraction

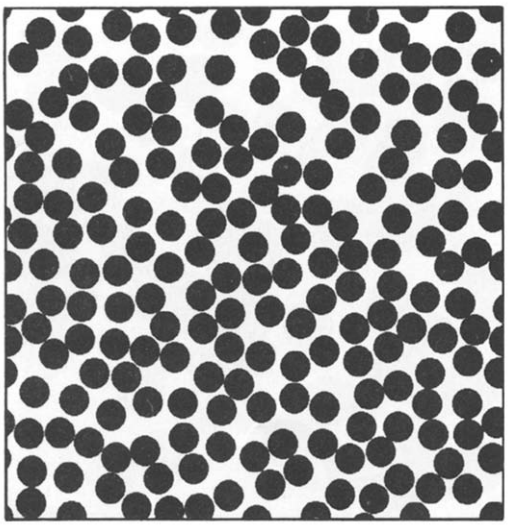

FIG 2 A computer-generated (512×512 pixels, $\simeq 750$ pixels per disk) configuration of hard disks ($\lambda = 1$, $R = 0.03$) near the RSA jamming limit ($\phi_2 \simeq 0.55$)

very near the RSA jamming limit. The case of fully penetrable disks ($\lambda = 0$) for $\phi_2 = 0.5$ is shown in Fig. 3. In generating media consisting of particles of arbitrary shape, the time required using the GRID method will not be significantly larger than the time needed to generate media composed of equi-sized disks (see simulation details below). This is not the case if the SC method is employed because the nonoverlap condition becomes considerably more difficult to test for particles of arbitrary shape.

As pointed out by Feder [24], the GRID method can lead to poor results for certain quantities (such as the jamming limit and the radial distribution function at contact) if a small number of pixels are used to represent each disk As shown in the subsequent section, the resolution employed in this study is sharp enough to give a very good estimate of the jamming limit.

For the GRID method, phase sampling is accomplished by bit testing. This is much faster than SC sampling, which requires floating-point calculations to determine if a test point is inside any of perhaps hundreds of disks. To speed sampling with the SC method, Haile, Massobrio, and Torquato [15] used a cell-list to reduce the number of distances to disk centers that must be calculated. (This is actually a hybridization of the SC method with the GRID method). They calculated S_2 for hard spheres using molecular dynamics simulations.

It is very easy to monitor the volume fraction of a configuration with the GRID method by a pixel count. With the SC method, configuration sampling after each disk addition is necessary.

In general, a surprisingly large amount of CPU time is spent on PBC since they must be applied during both configuration generation and sampling However,

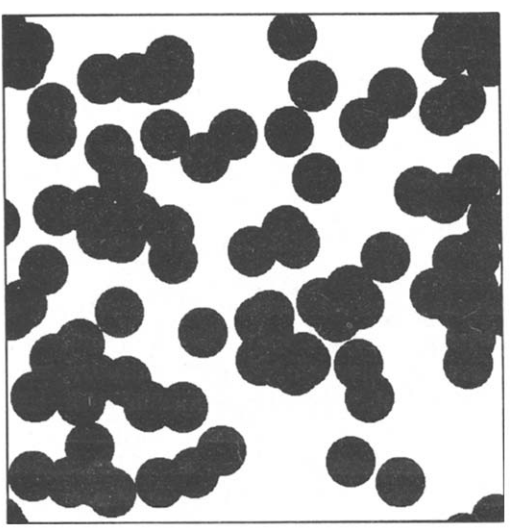

FIG 3. A computer-generated (512×512 pixels, $\simeq$2000 pixels per disk) configuration of fully penetrable disks ($\lambda = 0$, $R = 0.05$) at $\phi_2 \simeq 0.5$

PBC can be more quickly and simply handled using the GRID method than the SC method. The reason for this is described in simulation details given below.

B. *Simulation Details*

All simulations were performed using the GRID method (with PBC) on an IBM 4341 computer. Images of the inner (impenetrable) disks of radius λR and the outer concentric disks of radius R were stored in separate 256×128 INTEGER*4 arrays (32-bit integers, therefore 1024×1024 bits). Storing each image requires 128 Kb (1 Megabit). A multiplicative congruential random number generator with multiplier 16807 and modulus $2^{31} - 1$ was used both in configuration generation and sampling. This generator has good lattice statistics and relatively fast execution time [29].

The pixels along either axis are numbered 0, 1,. ..., $2^m - 1$ (We use $m = 10$). This numbering scheme permits a simple, rapid bit-masking algorithm for PBC to be used. For example, the pixel $(-200, 3000)$ is a replica of the pixel $(-200$ AND $1023, 3000$ AND $1023) = (824, 952)$. Bit testing and setting routines in the IBM VSFORTRAN library were used (BTEST, IBSET, IBCLR, ISHFT, IOR, and IAND).

If too small a value of m is used, small objects will become misrepresented (small disks will appear to be multisided polygons, for example). If too large a value of m is used, the pixel "painting" time per object during configuration generation as well as the memory requirements may become excessive. Sampling time is affected only if the increased memory requirements force a change of storage media.

The coordinates of the center of each prospective disk to be placed are generated using independent streams of random numbers. For convenience, the centers of all disks are centered on pixel sites. Because the impenetrable cores may not overlap in the PCS model, before placing any disk (except the first), we must test that its impenetrable core (of radius λR) does not overlap the core of a previously placed disk This is done by extracting a square "window" of pixels from the impenetrable core image. The prospective disk's core is first "AND-ed" onto the window. If there is overlap, not all bytes in the window will be zero, and a new disk center is generated and the process is repeated. A pixel count in the "penetrable" image is maintained at all times since the disk volume fraction is simply the ratio of the number of "1" pixels to the total number of pixels. Thus, a window is extracted from the "penetrable" image where the prospective disk would fall. The disk is "OR-ed" onto this window since overlap is allowed. The disk volume fractions with and without the new disk are compared to the desired disk volume fraction ϕ_2. Configuration generation is complete when the volume fraction without the new disk is closer to the desired ϕ_2 than with it included. (The tolerance on ϕ_2 varies with the resolution parameter m; we were able to generate configurations with an RMS error in ϕ_2 of less than 0.001 with $m = 10$.) Otherwise, the core disk is "OR-ed" onto its window, both windows are recopied into their respective images, and the volume fraction is updated. A new disk center is now generated and the entire process repeated

One advantage of the "windowing" technique is that PBC are applied only when the windows are copied from, or, if the disk is accepted, to the images. With the GRID method, to implement PBC it is not necessary to store anything outside the unit square; portions of a disk falling off an edge of the unit square wrap around to the opposite edge (see Figs. 2 and 3). Another advantage of the windowing technique is that it can be as easily applied to cases in which the particles have arbitrary shape. Hence, when the GRID method is utilized in conjunction with the windowing technique, the generation of media composed of arbitrary-shaped particles is not appreciably slower than that of media consisting of equi-sized disks.

$S_2(r)$ may be found by tossing line segments of length r at random orientations onto the "penetrable" images generated for a large number of representative configurations and measuring what fraction of the time both ends of the line segments fall in the matrix phase. A faster way of obtaining S_2 is to exploit the homogeneity and isotropy of the system by forming a "sampling template" to test, for example, 20 points arranged in a ring, equiangularly spaced at distance r from a random central point (see Fig. 4). A large number of sampling templates (say, 1000) are used to test each configuration.

For purposes of comparison, we carried out simulations using these two sampling techniques for distributions of fully penetrable disks (for which we have the exact result (8)) and of totally impenetrable disks at lower densities (which can be compared to the theoretical results of Torquato and Lado [17]). The method which makes use of the sampling template was found to give superior convergence to the known exact results because a much larger number of trials could be performed in a given time period. This becomes even more important when higher order S_n, such as S_3 are to be simulated and integrated—a subject of a future study.

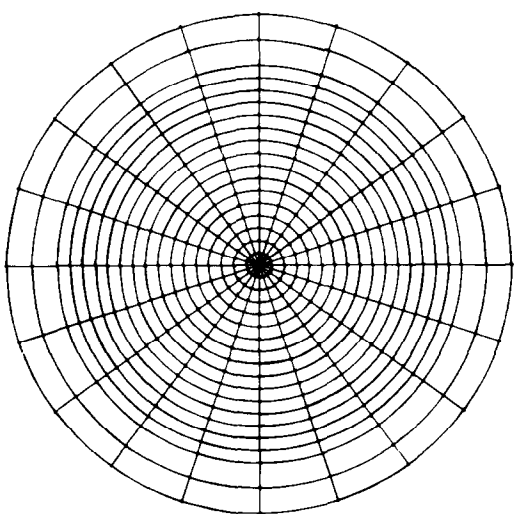

FIG 4 Sampling templete to test for S_2

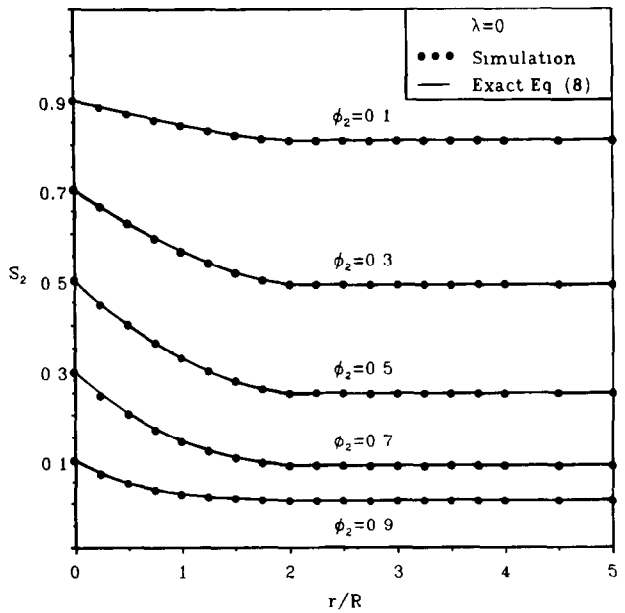

FIG 5 A comparison of RSA simulation results for S_2 in the PCS model for fully penetrable disks ($\lambda = 0$) to the exact results obtained from Eq (8), for $\phi_2 = 0\,1$, $0\,3$, $0\,5$, $0\,7$, and $0\,9$ The points are the simulation data and the curves are the exact results

TABLE I

RMS Deviations of Simulation Results for the Cases $\lambda = 0$ and $\lambda = 1$ from Corresponding Theoretical Results (Eq (8) and Ref [17], respectively)

	RMS Deviation	
ϕ_2	Fully penetrable disks $\lambda = 0$	Totally impenetrable disks $\lambda = 1$
0 1	0 000618	0 000431
0 2	—	0 000763
0 3	0 000434	0 001356
0 4	—	0 001663
0 5	0 000952	0 002333
0 7	0 001553	—
0 9	0 000187	—

Accordingly, we compute S_2 using the faster sampling method. The mean CPU time to test 1000 sampling templates was 10 s.

IV. Results and Discussion

In Figs. 5–9, we present $S_2(r)$ for distributions of disks in the PCS model for $\lambda = 0$, 0.5, 0.7, 0.9, and 1, respectively, at selected values of the disk volume fraction ϕ_2. A total of 1000 sampling templates were employed to test each of 100 configurations for all ϕ_2, except the jamming-limit value. Only 20 configurations were used for the jamming-limit cases.

For the instance of fully penetrable disks ($\lambda = 0$), Fig. 5 also includes exact results as obtained from Eq. (8). The RMS deviations from the exact results are presented in Table I. It is seen that the agreement between simulation and exact results is excellent; the largest RMS relative deviation being 0.16 % at $\phi_2 = 0.7$.

At the opposite extreme of totally impenetrable disks ($\lambda = 1$), we compare our RSA simulation results to the theoretical results of Torquato and Lado [17] for an equilibrium distribution of such disks (Fig. 9) The calculation of S_2 in Ref. [17] involves an integral over, among other quantities, the radial distribution function $g(r)$ Included in Table I is the RMS deviation from the Torquato–Lado results.

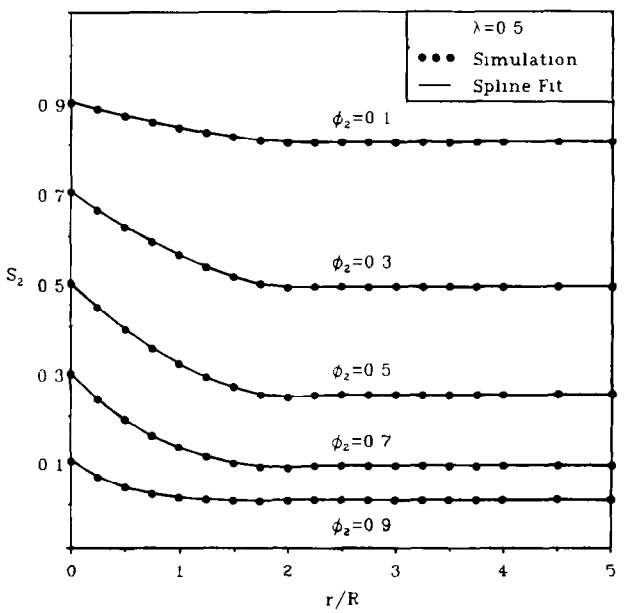

FIG 6 RSA simulation results for S_2 in the PCS model for an impenetrability parameter $\lambda = 0.5$ at selected values of the disk volume fraction ϕ_2 The points are the simulation results and the curves are spline fits

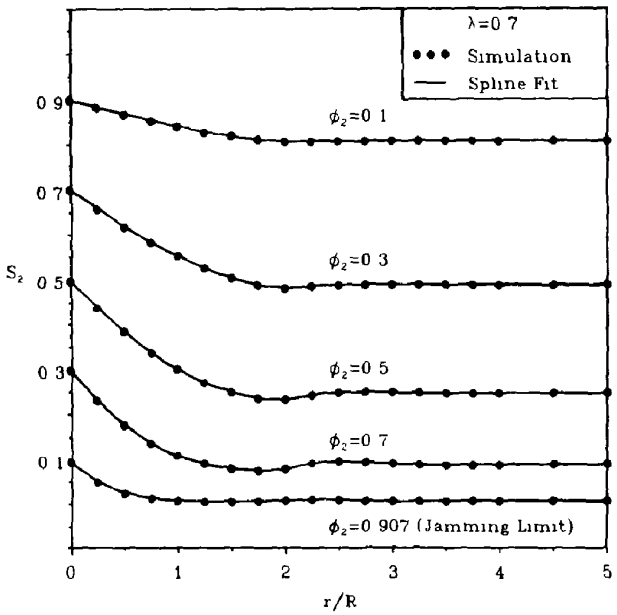

FIG 7 As for Fig 6, with $\lambda = 0\,7$

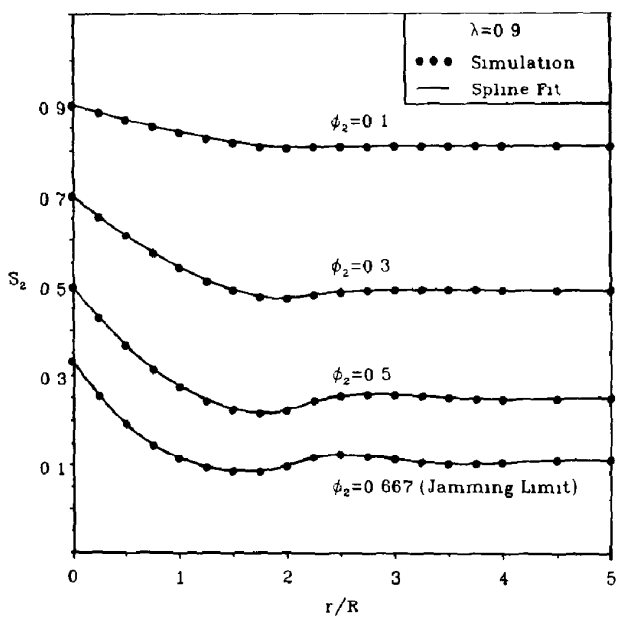

FIG 8 As for Fig 6, with $\lambda = 0\,9$

Interestingly, the agreement between the equilibrium and our RSA results is excellent, even at high particle densities at which the respective radial distribution functions are distinctly different [24, 30]. Clearly, the averaging process of integration over $g(r)$ is the reason why S_2 is insensitive to differences between the equilibrium and nonequilibrium (RSA) distributions for $\lambda = 1$. Note that the RSA results presented in Fig. 9 are new. $S_2(r)$ is a damped, oscillating function, oscillating about its long-range value of ϕ_1^2 with an amplitude that becomes negligible on the scale of our figures after several diameters: as indication of some short-range order. As the density of disks is increased, the correlation length (defined to be the distance at which $(S_2(r) - \phi_1^2)$ becomes negligible) is seen to increase. By contrast, the corresponding $S_2(r)$ for $\lambda = 0$ (Fig. 5) is seen to exponentially decay to ϕ_1^2 when $r = 2R$, and remains equal to ϕ_1^2 for $r > 2R$: an indication of the total absence of any spatial correlation.

In Figs. 6–8 we present, for the first time, results for $S_2(r)$ at the intermediate values $\lambda = 0.5, 0.7, 0.9$, respectively. We also obtained, but do not report, results for cases in the range $0 < \lambda < 0.5$. For $0 < \lambda < 0.5$, S_2 was negligibly different than S_2 for fully penetrable disks ($\lambda = 0$) at the same ϕ_2. Thus, even though exclusion volume effects increase (i.e., although the amplitude in the oscillations of $g(r)$ increase) as λ is made to increase, S_2 is not sensitive enough to reflect these microstructural

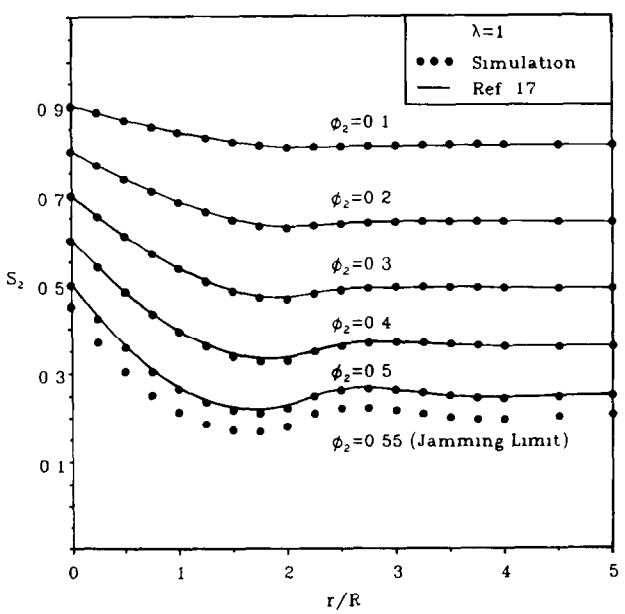

FIG 9 A comparison of RSA simulation results for S_2 in the PCS model for totally impenetrable disks ($\lambda = 1$) to the corresponding equilibrium results of Torquato and Lado [17], for $\phi_2 = 0.1, 0.2, 0.3, 0.4$, and 0.5 The simulation of S_2 at the jamming limit ($\phi_2 \simeq 0.55$) is also included The points are the simulation results and the curves are equilibrium results.

differences in the range $0 < \lambda < 0.5$. The general reason for this has already been noted. For $0.5 \leqslant \lambda < 1$, the amplitude of the oscillations in S_2 for constant ϕ_2 increases as λ increases, as expected. It is only when λ is near unity ($\lambda \geqslant 0.9$) that one can detect appreciable oscillations in S_2.

Note that for the cases $\lambda = 0.7$, 0.9, and 1 (Figs. 7–9), we also computed the corresponding jamming-limit volume fraction ϕ_2. For example, using the GRID method, we found that the jamming limit occurred at $\phi_2 \simeq 0.55$ for $\lambda = 1$. This calculation involved 20 configurations, 10^7 attempts to place disks per configuration, and approximately 200 disks per configuration. Feder [24], using the SC method, found the jamming limit occurred at $\phi_2 \simeq 0.547$. Feder used 30 configurations, 10^8 attempts, and approximately 2700 disks per configuration. In earlier work, Finegold and Donnell [31] reported $\phi_2 \simeq 0.5$. They used the GRID method (1024×1024 pixels), but used disks about one-half the size we used ($R \simeq 0.014$). In light of the accuracy we achieved, we believe the disk size, and not the GRID method, as Feder suggests, were responsible for the lower value calculated by Finegold and Donnell.

Lastly, in Fig. 10, we present results for the specific surface s for $\lambda = 0$, 0.5, 0.7, 0.9, and 1 (at selected ϕ_2) as computed from Eq. (6) and our simulations. For $\lambda = 0$ and $\lambda = 1$ our results may be compared to the exact results $s = 2\eta\phi_1/R$ and $s = 2\phi_2/R$, respectively. The RMS deviations are, respectively, 0 77 % and 1.33 %

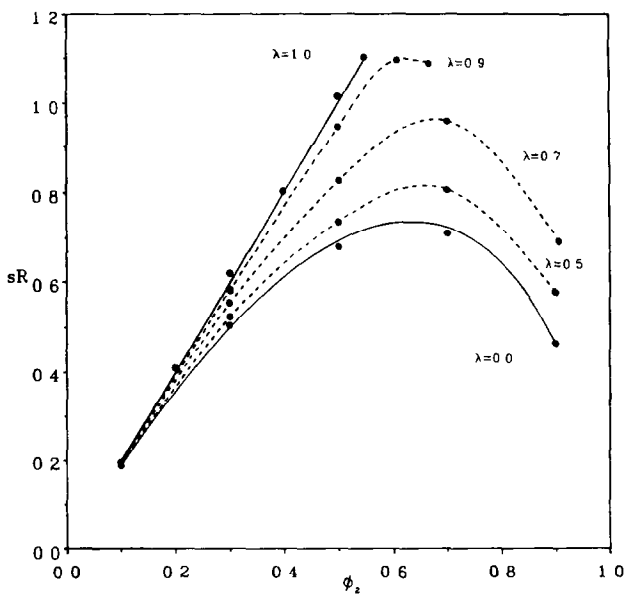

FIG 10 The reduced specific surface sR versus ϕ_2, as calculated from the simulation results (points) using Eq (6), for $\lambda = 0$, 0.5, 0 7, 0.9, and 1 Solid lines for $\lambda = 0$ and $\lambda = 1$ are exact results. Dashed lines for $\lambda = 0.5$, 0 7, and 0 9 are spline fits Note that for $\lambda = 0\,9$, we report sR for $\phi_2 = 0\,61$, a volume-fraction value not given in Fig 8

(Note that numerical differentiation of simulation results causes error magnification.) The results given for $\lambda = 0.5$, 0.7, and 0.9 are new. As expected, s monotonically increases as the impenetrability parameter λ increases at constant ϕ_2.

V. Concluding Remarks

Our results for S_2 in the special limits $\lambda = 0$ (fully penetrable disks) and $\lambda = 1$ (impenetrable disks) show excellent agreement with previous work, as does our prediction of the jamming limit volume fraction for random sequential addition at $\lambda = 1$. This validates the methods used for generating and sampling representative configurations of synthetic disordered media. It was shown that these methods may be applied to media consisting of particles of arbitrary shape. Although we focused our attention on 2D media, the simulation techniques reported in this study can be easily extended to 3D media.

Moreover, we report, for the first time, results for S_2 and the specific surface s at intermediate values of the impenetrability parameter λ in the PCS model. As λ increases (i.e., as the radius of the inner hard core increases), the amplitudes of the oscillations in S_2 become more pronounced, as expected. For $0 < \lambda < 0.5$, however, S_2 is virtually insensitive to λ, behaving (to a good approximation) as the corresponding two-point function for fully penetrable particles ($\lambda = 0$).

The high-speed sampling method outlined is well suited to prediction of higher order S_n such as S_3 and, in addition, is independent of the shape of the inclusions and any penetrability constraints. In subsequent papers, we shall employ this sampling technique to compute S_3 and bounds on bulk properties which depend on S_3 for distributions of disks and ellipses.

Acknowledgment

The authors gratefully acknowledge the support of the Office of Basic Energy Sciences, U S Department of Energy, under Grant DE-FG05-86ER13482

References

1 See, e.g, S Torquato, *J. Stat Phys* **45**, 843 (1986), and references therein
2. G W Milton, *J Appl Phys.* **52**, 5294 (1981)
3. S Torquato, *J Appl. Phys* **58**, 3790 (1985)
4 G. W Milton, *J. Mech. Phys. Solids* **30**, 177 (1982)
5 N Phan-Thien and G W Milton, *Proc. Roy Soc London A* **380**, 305 (1982)
6 S Prager, *Phys. Fluids* **4**, 1477 (1961), R A Reck and S Prager, *J Chem Phys* **42**, 3027 (1965)
7 M Doi, *J. Phys. Soc. Japan* **40**, 567 (1976).
8. J G Berryman and G. W Milton, *J. Chem Phys.* **82**, 754 (1985)
9 S Torquato and G Stell, *J Chem Phys* **77**, 2071 (1982).
10 S Torquato and G Stell, *J Chem. Phys* **78**, 3262 (1983).

11 S TORQUATO AND G STELL, *J Chem Phys* **79**, 1505 (1983)
12 S. TORQUATO AND G STELL, *J Chem Phys* **80**, 878 (1984)
13 S TORQUATO AND G STELL, *J Chem Phys* **82**, 980 (1985).
14 J G. BERRYMAN, *J Appl Phys* **57**, 2374 (1985)
15 J M. HAILE, C MASSOBRIO, AND S TORQUATO, *J Chem Phys.* **83**, 4075 (1985).
16 In the article, N A SEATON AND E D. GLANDT, *J. Chem. Phys.* **85**, 5262 (1986), the authors use a Monte Carlo method to compute two-point correlation functions (involving interfacial information) different from but related to S_2 The relationships between these different two-point functions is discussed in full detail in Ref [1]
17 S TORQUATO AND F LADO, *J Phys A Math Gen* **18**, 141 (1985)
18 S TORQUATO, *J Chem Phys* **81**, 5079 (1984), S TORQUATO, *J Chem Phys* **84**, 6345 (1986)
19 S TORQUATO, *Rev Chem Eng* **4**, 151 (1987)
20 P DEBYE, H R ANDERSON, JR , AND H BRUMBURGER, *J Appl Phys* **28**, 679 (1957)
21 J G. BERRYMAN AND S C. BLAIR, *J Appl Phys.* **60**, 1930 (1986)
22 S TORQUATO AND J D BEASLEY, *Int. J Eng Sci* **24**, 415 (1986)
23 B WIDOM, *J Chem Phys* **44**, 3888 (1966)
24 J FEDER, *J Theor Biol* **87**, 237 (1980)
25 This jamming limit value ($\phi_2 \simeq 0.55$) is also computed in the present study using the GRID method.
26 The volume fraction $\phi_2 \simeq 0.82$ corresponds to the random close-packing value (see, e g, J G BERRYMAN, *Phys Rev A* **27**, 1053 (1983)), which for an equilibrium distribution of rigid disks is a metastable disordered (i.e, glassy) state
27 N METROPOLIS, A W ROSENBLUTH, M N ROSENBLUTH, A H TELLER, AND E TELLER, *J Chem Phys* **21**, 1087 (1953)
28 B J. ALDER AND T E WAINWRIGHT, *J Chem Phys* **31**, 459 (1959)
29 G S FISHMAN AND L R MOORE, *J Amer Stat Assoc* 77, 129 (1982)
30 In the dilute limit, the RSA and equilibrium radial distribution functions are identical (see Ref [23]), and hence the corresponding two-point functions are the same in this limit.
31 L FINEGOLD AND J T DONNELL, *Nature* **278**, 3262 (1983)